

AD-A125 046

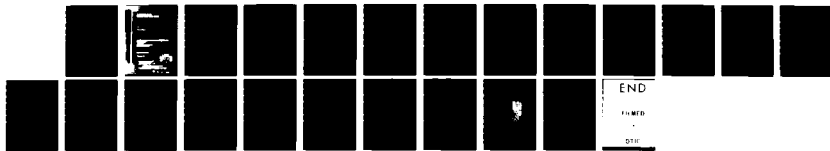
A DYNAMIC MODEL FOR THE TRANSITION REGION(U) STANFORD  
UNIV CA INST FOR PLASMA RESEARCH S K ANTIOCHOS NOV 82  
SUIPR-947 N00014-75-C-0673

1/1

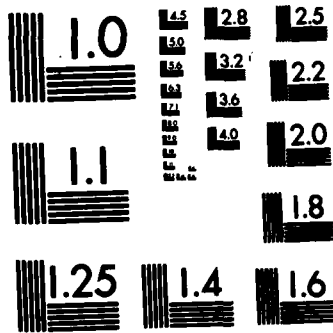
UNCLASSIFIED

F/G 3/2

NL



END  
FILMED  
DTIC



MICROCOPY RESOLUTION TEST CHART  
NATIONAL BUREAU OF STANDARDS-1963-A

AD A1 25046

**A DYNAMIC MODEL FOR THE TRANSITION REGION**

**S. K. Antiochos  
Institute for Plasma Research  
Stanford University  
Stanford, CA 94305**

Author: S. K. Antiochos  
NRLS: 1224  
DTIC: 1224

*Letter on file*

DTIC  
COPY  
INSPECTED  
2

*A*

### Abstract

We develop a model for the lower transition region,  $10^{4.3} \leq T \leq 10^{5.3}$ , that can account for the persistent and ubiquitous redshifts that are observed in the UV emission lines formed at these temperatures. We show that these shifts are not likely to be due either to falling spicular material or to steady-state siphon flows. Our model consists of two key ingredients. (a) The redshifted radiation originates from a minority of flux tubes which have higher gas pressures than their surroundings, and consequently have their transition regions situated below the transition regions of their surroundings. (b) The coronal heating in these loops is impulsive in nature, and this is responsible for the transient mass flows. Our studies, therefore, favor theories for coronal heating which involve flare-like magnetic-energy release.

## I. Introduction

From observations of UV emission lines, the structure inferred for the lower transition region,  $10^{4.3} \leq T \leq 10^{5.3}$  K appears to exhibit several curious features. First, persistent redshifts, but not blueshifts, are observed in lines originating from all types of solar regions: coronal holes, quiet sun and active regions (e.g., Doschek, Feldman and Bohlin 1976, Lites et al. 1976, Gebbie et al. 1981, Dere 1982); and also from all solar-type stars for which observations of sufficient quality to detect such redshifts are available (Ayres et al. 1982). These redshifts indicate velocities of  $\sim 10$  km sec<sup>-1</sup>. A key result is that the redshifts are observed out to, but not above, the limb with little change from disk center to limb (Feldman, Cohen and Doschek 1982). The shifts disappear for material hotter or cooler than  $\sim 10^5$  K.

Another interesting feature is the form of the differential emission measure in this temperature range. The observed form is not compatible with static models such as the so-called "quasi-static" models of coronal loops (e.g., Vesecky, Antiochos and Underwood 1979). Although the static models can account for the differential emission measure in the upper transition region and corona,  $T > 10^5$ , they fail to reproduce the observed steep increase in emission measure for  $T < 10^5$  (Pallavicini et al. 1981, Athay 1981). The observations indicate that in the lower transition region of the sun and of other solar-like stars,  $q \propto T^{-\delta}$  with  $\delta \sim 2-3$  (e.g., Doschek et al. 1978, Raymond and Doyle 1981, Saxner 1981, and Zolcinski et al. 1982), where for a loop geometry the differential emission measure  $q$  is defined as:

$$q(T) = A n^2 T \left| \frac{\partial T}{\partial s} \right|^{-1} \quad (1)$$

and  $A$  is the cross-sectional area of the loop,  $n$  is the electron density, and  $\partial T / \partial s$  is the temperature gradient along the loop, i.e., parallel to the magnetic field. Since persistent redshifts are observed in this temperature

range, it is natural to consider whether models with steady-state flows can account for the form of  $q$ , but these models (at least for a single loop) also fail to produce a sufficiently rapid increase in  $q$  at low temperature (e.g., Athay 1981).

It should be noted, however, that this result on the form of  $q$  is suspect. Shoub (1982) has shown that kinetic effects, which have not been included in all the models to date, are likely to be important in the lower transition region. In this case the interpretation of the observed UV line fluxes in terms of a simple differential emission measure is incorrect. For this reason we will concentrate in this paper primarily on the redshift observations rather than on the form inferred for  $q$ .

We believe that the observed features described above have highly important implications, not only for the structure of the lower transition region, but for the corona in general. In the next sections we discuss these implications and derive a model that may account for the observations.

## II. Implications of the Redshifts

The observation of persistent redshifts on the limb (Feldman, Cohen and Doschek 1982) is very puzzling, and it imposes severe constraints on the geometry of the emitting region. For example, it rules out the possibility that the observed emission is due to downflowing material in a simple loop. Since the plasma in the solar corona and transition region is constrained to move along the magnetic field, the doppler shift observed from moving material depends on the angle between the line of sight and the magnetic field. If the emission is from a single loop, i.e., the field lines are all parallel, then the doppler shifts should change dramatically depending on whether the loop were on the disk or limb. In particular, assuming that the field is exactly vertical to the solar surface, then on the disk, redshifts would be observed

from downward flowing material; however, on the limb no shifts would be observed from this material since the line of sight would be transverse to the plasma velocity. In general, we would expect that the magnetic field emerges from the solar surface at some finite angle to the vertical, so that at the limb, downward motion would result in an observable doppler shift. However, these shifts would be as likely to be blue as red; hence, again we would expect no net lineshifts at the limb.

Note that this result argues strongly against the suggestion that the observed redshifts are due to spicular material that is falling back onto the chromosphere (e.g., Pneuman and Kopp 1977, 1978; Poletto 1981; Athay 1981; Athay and Holzer 1982). Downflowing material, by itself, is not sufficient to explain redshifts at the limb. If the shifts were, indeed, due to falling spicular material, we would expect to observe a strong center-to-limb variation in the redshifts. But this is not the case (Feldman, Cohen and Doschek 1982). In addition, since spicules extend well above the solar surface,  $\geq 10^4$  km, one would not expect the shifts to disappear above the limb, as is observed. The observations suggest that the shifts actually originate from below the surface.

We propose that this is, indeed, the explanation for the limb shifts. We believe that they are due to downflowing material in the lower transition region at the base of high-pressure coronal loops. The limb shifts can be understood quite readily by the simple geometry illustrated in Figure 1. Consider a flux tube in which the magnetic field enters the solar surface at a small angle. In this picture the solar surface is taken to be the top of the chromosphere, which is defined as the level at which  $T \sim 10^{4.3}$  K. Assume that, as is accepted, the magnetic field dominates the plasma so that there can exist large variations in plasma pressure across the field. Also, since the thermal conductivity perpendicular to the field is many orders of magni-

tude smaller than the parallel conductivity, there can exist large variations in plasma temperature across the field. If the plasma pressure inside the flux tube is larger than in the surrounding region, then we expect that the top of the chromosphere occurs at a lower height than in the surrounding region. The difference in height will be of the order of the gravitational scale height in the chromosphere,  $H_g \sim 10^{7.5}$  cm. for  $T \sim 10^4$  K. However, the temperature scale height in the lower transition region is typically much less than this. For example, in the static models of coronal loops, the temperature scale height,  $H_T$ , along the loop is given by (Vesecky, Antiochos and Underwood 1979):

$$H_T(T) \sim L (T/T_{COR})^3, \quad (2)$$

where  $L$  is the loop length and  $T_{COR}$  is the maximum temperature in the loop. For average loop lengths,  $L \sim 10^9$  cm., and coronal temperatures,  $T_{COR} \sim 10^{6.3}$  K, we find that  $H_T(10^5) < 10^6$  cm. This simply restates the well-known result that the transition region is extremely thin compared to the size of the corona or chromosphere.

Hence, we conclude that the lower transition region in a high-pressure loop is located at the bottom of a deep "well" formed by surrounding low-pressure chromospheric material, as is illustrated in Figure 1. The key point of this picture is that any emission from the bottom of the well will be observable only if the line of sight forms a relatively small angle to the magnetic field direction, i.e., the observer must be looking down the well. If the lower transition region material is flowing down, then only redshifts will be observed. This can be seen from Figure 1. Observer A's line of sight is approximately along the field, and hence he observes redshifted emission; whereas observer B, who would normally observe blueshifts, sees no emission

since it is obscured by the intervening chromospheric material.

The amount of intervening material required to obscure the emission is only of the order of the well depth. Calculations by Vernazza, Avrett and Loesser (1981) indicate that  $\sim 10^8$  cm. of quiet chromosphere is sufficient to produce optical depth unity in the wavelength range of the observed redshifted lines: 1200 - 1400 Å. Therefore, the angle to the magnetic field direction at which obscuration sets in can be quite small. It depends on the ratio,  $W/H_g$ , of the width of the loop to the gravitational scale height, i.e., the width of the well to its depth. Our model is most effective if this ratio is of order unity; since if  $W/H_g \gg 1$ , then the amount of obscuration becomes negligible and, on the other hand, if  $W/H_g \ll 1$ , the obscuration is so effective that the observable emission from the base of the high-pressure loops becomes negligible.

Assuming that  $W/H_g \approx 1$  implies that the obscuration angle  $\approx 45^\circ$ . Hence, if the direction of the magnetic field is uniformly distributed, we expect to observe emission from  $\sim 30\%$  of the high-pressure loops in a particular area near disk center, and  $\sim 15\%$  near the limb. The observations (Feldman, Cohen and Doschek 1982) do, in fact, show a decrease by a small factor,  $< 2$ , in the magnitude of the redshifts from center to limb. Of course, the area covered by these loops is only a fraction of the area observed, say,  $\sim 10\%$ . In this case the emission per unit area from the high-pressure loops must be  $\geq 50$  times that of the low-pressure material for the redshifted emission to contribute significantly. We believe that this condition is easily satisfied since both the density is higher in the high-pressure loops and, as we show below, the temperature structure of the downflowing material tends to enhance the emission.

Note that above the limb no obscuration is possible, so that by the arguments presented previously, redshifts are not expected even if all the

material at lower transition region temperatures is flowing downward. This provides a straightforward explanation for the observation that the redshifts disappear abruptly above the limb.

In addition, our model provides a natural explanation for the observation that solar UV lines formed throughout the disk indicate absorption by cooler neutral material (Schmahl and Orrall 1979; Doschek and Feldman 1982). Observer C in Figure 1, who would correspond to observing at disk center, sees absorption from the chromospheric material lying above the transition region of the high-pressure flux tube.

### III. Steady-State Flow

The model presented in the previous section can account for the observation of line shifts, even near the limb, but the question remains as to why the observed shifts are red rather than blue. On the average, at least as much material flows up from the solar surface as flows down; in fact, slightly more must flow up to provide the solar wind loss. Therefore, there must be both blue- and redshifted emission, and there is no reason, a priori, to expect that the redshifts dominate.

In order to determine the relative strengths of the red- and blueshifts, a definite model is needed for the flows. One possibility is that they are steady-state siphon flows, i.e., driven by a temperature difference between the two ends of a loop. Such flows have been discussed by a number of authors (e.g., Cargill and Priest 1980; Glencross 1980; and Landini and Fossi 1981). It turns out, however, that the steady-state flows result in predominantly blueshifted emission.

Consider a simple model for steady-state flow in which we assume a loop of constant cross-section, neglect the effect of gravity and assume that the coronal heating is a function of temperature and density only. We also

neglect the kinetic effects described by Shoub (1982) so that a fluid description for the plasma is valid. In addition, we assume that the velocities are sufficiently small and the densities sufficiently high that ionization nonequilibrium effects (e.g., Borrini and Nocci 1982) are not significant. The fluid equations in this case reduce to:

$$\rho v = J \quad (3)$$

$$\rho v^2 + p = H \quad (4)$$

$$d/ds (1/2 \rho v^3 + 5/2 p v - 10^{-6} T^{5/2} dT/ds) = -n^2 \Lambda(T) + \epsilon(n, T) \quad (5)$$

where:  $\rho$  is the mass density,  $v$  is the plasma velocity,  $p$  is the total pressure,  $\Lambda(T)$  is the radiative loss coefficient for optically thin plasma (e.g., Raymond, Cox and Smith 1976),  $n$  is the electron density,  $\Lambda$  is the coronal heating function, and we have used the thermal conductivity given by Spitzer (1962). The quantities  $J$  and  $H$  are constants, and represent the mass flux and momentum flux, respectively.

Assuming that the loop is at the center of the disk so that geometrical effects do not favor observing one side of the loop over the other, then any UV line observed from the loop will consist of two components, a blueshifted contribution from that leg of the loop where material is flowing up, and a redshifted contribution from the downflowing leg. The wavelength shift inferred for such a line will, in general, depend on the detailed shape of each component and on the method of analysis used. However, for the purposes of making a simple comparison of the relative strengths of each component, let us assume that each makes a contribution  $\Delta\lambda$  to the inferred shift that is proportional to the doppler shift of the component and to its intensity; hence,

$$\Delta\lambda_{u,d} \propto v_{u,d}(T) n_{u,d}^2(T) T |dT/ds|_{u,d}^{-1} \quad (6)$$

where the subscripts "u" and "d" refer to the upflowing (blueshifted) and downflowing (redshifted) material, respectively; and we have used the fact that the line intensity is proportional to the differential emission measure as defined in equation (1). From (6), the ratio of the blue to red shifts is:

$$\frac{\Delta\lambda_u}{\Delta\lambda_d} = \frac{v_d |dT/ds|_d}{v_u |dT/ds|_u} \quad (7)$$

where we have used equation (3) to eliminate the density dependence. If the flows are subsonic, then equations (3) and (4) and the equation of state can be used to determine  $v$  as a single-valued function of  $T$ , viz:

$$v(T) = H/2J - [(H/2J)^2 - 2kT/m]^{1/2}, \quad (8)$$

where  $k$  is Boltzmann's constant,  $m$  is the hydrogen mass, and we have selected the coordinate system so that  $v$  and, hence,  $J$  are positive.

In this case,  $v_d(T) = v_u(T)$ , and the ratio depends only on the temperature gradient at the two regions where the line is formed, equation (7). Although this result is strictly valid only for the simple model described here, we believe that it is generally true that the difference between the emissions from the upflowing and downflowing material is due primarily to a difference in the temperature gradients rather than the densities or velocities. This is because differences in the velocity and density are restricted by the constraints that the average upward mass flux must equal the average downward flux and that the velocities are unlikely to be much larger than the sound speed. Hence, we believe it is unlikely that the velocities and densities can differ by orders of magnitude between the upflowing and downflowing material. The temperature gradients, on the other hand, are very sensitive to

the physical model and can differ by orders of magnitude, especially at such low temperatures. This is certainly true for the models for flare cooling (e.g, Antiochos 1981).

In order to obtain the temperature gradients predicted by the steady-state model, we transform from  $s$  to  $T$  as the independent variable in the energy equation (5) and use (3) and (8) to express  $v$  and  $\rho$  (or  $n$ ) as functions of  $T$ :

$$\begin{aligned} d/dT (T^5 [dT/ds]^2) &= 2 \times 10^6 T^{5/2} (n^2(T) \Lambda(T) - \epsilon(T)) \\ &+ 10^6 (k/m) HT^{5/2} [8J/H + ((H/2J)^2 - 2kT/m)^{-1/2}] dT/ds \end{aligned} \quad (9)$$

The important point of equation (9) is that the first term on the RHS, which represents the effects of the radiative losses and coronal heating, is a function of  $T$  only, whereas the last term, which represents the effects of mass motion, is proportional to the temperature gradient. Therefore, the difference in the temperature gradient between the upflowing and downflowing legs of the loop is due only to the second term. This can be seen immediately by formally solving (9) for  $dT/ds$ . Letting  $T_{\text{cor}}$  be the maximum temperature in the loop, we obtain:

$$\begin{aligned} (dT/ds)^2 (T) &= 2 \times 10^6 T^{-5} \int_T^{T_{\text{cor}}} (\epsilon - n^2 \Lambda) T^{5/2} dT \\ &- 10^6 (k/m) HT^{-5} \int_T^{T_{\text{cor}}} [8J/H + ((H/2J)^2 - 2kT/m)^{-1/2}] dT/ds T^{5/2} dT \end{aligned} \quad (10)$$

Equation (10) is the important result of the steady-state flow model. It shows that the blueshifts dominate the red. Since we have picked our coordinate system so that  $J$  is positive, in the upflowing leg  $dT/ds$  is positive, but

in the downflowing leg  $dT/ds$  is negative. Hence, at any temperature  $T$ , the square of the temperature gradient in the downflowing leg is larger than the square of the gradient in the upflowing leg. The difference is simply equal to twice the second integral in the RHS of (10). In Figure 2 we plot  $(dT/ds_d)/(dT/ds_u)$  for a model loop with the particular values for the adjustable parameters:  $T_{\text{cor}} = 10^6$  K,  $H = 2$  ergs. cm.<sup>-3</sup>,  $J = 5 \times 10^{-8}$  gm. cm.<sup>-2</sup> sec.<sup>-1</sup> and  $\epsilon(n,T) = \text{constant} = 0.56$  ergs cm.<sup>-3</sup> sec.<sup>-1</sup>. These values imply a loop pressure of 1.8 erg cm.<sup>-3</sup> and a velocity of 4.2 km sec.<sup>-1</sup> at  $10^5$  K. We note from the figure that at  $10^5$  K, where the UV lines are formed,  $dT/ds_d \approx 15$   $dT/ds_u$  and, hence, the blueshifted component dominates by a factor of  $\sim 15$ . We conclude, therefore, that steady-state flows would produce blueshifts rather than the observed redshifts.

Of course, we have only shown this result for the simple model described here. It may be possible that by including complications such as a variable loop area, gravity or a spatially dependent energy input, one will be able to produce steady-state models in which the redshifts dominate. We are presently investigating models with these effects; however, our feeling is that, in general, steady flows will tend to favor blueshifts over red. The physical reason for this result is that in the upflowing leg of a loop, material is being accelerated, and hence the mass motions act as a heat sink; but, in the downflowing leg, material is decelerating and acting as a heat source. Therefore, the mass motion can be thought of as increasing the energy input to the loop on the downflowing side and decreasing it on the upflowing side. Since the downward conductive flux on either side of the loop is essentially the difference between the energy input and the energy lost by radiation, it will be larger on the downflowing side, where the effective energy input is larger. However, the temperature gradient is proportional to the heat flux and, so,

should be larger on the downside, resulting in decreasing emissions from this side. Note that gravity only enhances this argument because it also acts as an energy sink on the upside and a source on the downside.

There are other difficulties with the steady-state model. One is that it fails to reproduce the observed steep increase in the differential emission measure at low temperature (e.g., Pneuman and Kopp 1978, Athay 1981); however, as stated previously, this may be due to the neglect of kinetic effects in the model (Shoub 1982).

Another difficulty is the form of the velocity profile. From the observed redshifts of lines formed at different temperatures, it appears that the velocity has a sharp peak at  $T = 10^5$  K (Dere 1982). However, for steady-state flow the mass flux  $\rho v A$  is a constant and since the cross-section  $A$  must be approximately constant through the very narrow transition region, a sharp peak in the velocity must imply a sharp minimum in the density and pressure at  $T = 10^5$  K. We see no mechanism by which such a profile can be produced in a steady-state model, and there is certainly no evidence in the observations for a density and pressure minimum at  $T = 10^5$  K. It seems clear that in order to produce the observed velocity profile, time-dependent flows are required. We discuss such flows in the next section.

#### IV. Transient Flows

The most probable mechanism for producing mass motions in the corona and transition region is a transient coronal heating. In order for significant flows to develop, the time scale for variations of the energy input must be less than or of the order of the coronal cooling time  $\sim 10^3$  sec. The flows in this case are essentially identical to those believed to occur in a flare: chromospheric evaporation (Antiochos and Sturrock 1978) during the rise phase and coronal condensation (Antiochos and Sturrock 1982) during the cooling.

Even if the coronal heating is constant, it is still possible for flows to occur due to thermal instability (Antiochos 1979, Antiochos et al. 1982). However, we believe that this is a less likely mechanism for explaining the observations since it is clear that the temperature gradients inferred from the observations are very different from those of the static model and the plasma velocities are sizable. Hence, the amplitude of the instability would have to become very large in the nonlinear regime. We will discuss the nonlinear development of thermal instability in coronal loops in a future article.

A key aspect of transient coronal heating is that it naturally leads to the result that the UV emission during the downflowing stage should dominate the emission during the upflowing. This can be seen from the following arguments: Consider a coronal loop that is initially static with a pressure  $P_0$  and coronal heating rate  $\epsilon_0$ . If the energy input rises suddenly to a new value  $\epsilon$ ,  $\gg \epsilon_0$ , the loop will respond by evaporating chromospheric material until after a time,  $\tau$ , it reaches a new equilibrium state with pressure  $P$ ,  $\gg P_0$ . During this period blueshifted UV emission will occur; however, we expect that the total UV energy emitted  $E_b(\text{UV}) \ll (\epsilon - \epsilon_0)\tau$  since, during the evaporative phase, conduction dominates radiation and most of the energy input goes into mass motion (Antiochos 1981). This is what drives the evaporation in the first place. In fact, it can be shown that the initial effect of increasing  $\epsilon$  very rapidly is to decrease the transition region radiation because initially the coronal temperature and, hence the downward heat flux rise, whereas the loop density does not increase until some evaporation has occurred. A larger heat flux implies larger temperature gradients and a decrease in the differential emission measure. We expect, therefore, that the "excess" energy  $(\epsilon - \epsilon_0)$  that is available for blueshifted radiation instead

ends up primarily as the increased thermal energy in the loop  $(P - P_0) V$ , where  $V$  is the loop volume.

Now assume that the energy input drops back to its original value  $P_0$ . There is now an excess of thermal energy,  $(P - P_0) V$ , in the loop. The results of Antiochos and Sturrock (1982) imply that a significant fraction of this excess energy may be dissipated by radiation from low-temperature plasma,  $T < 10^6$  K. The coronal energy is transferred to the lower transition region and chromosphere by a large downward enthalpy flux which can dominate both the downward conductive flux and the coronal radiation. In this case, the total energy emitted as redshifted UV radiation,  $E_r$  (UV) can be of the order of the excess loop energy,  $(P - P_0) V$ . Since  $(P - P_0) V - (\epsilon - \epsilon_0)\tau \gg E_b$  (UV), we conclude that  $E_r$  (UV)  $\gg E_b$  (UV).

Of course, these arguments are only qualitative. In order to compare this model with the data, a detailed numerical simulation is required of the response of the corona and transition region to transient heating. Unfortunately, this is very difficult due to the problems of numerically resolving the transition region (Antiochos and Krall 1979) and treating the chromospheric response properly, which requires an accurate treatment of optically thick radiation losses. (However, a numerical model that may be able to handle these problems has recently been developed by McClymont and Canfield (1982).) The important point of the qualitative arguments above is that simple considerations lead one to expect that the redshifted emission should dominate the blue for a transiently heated loop. Note that, again, we expect the main difference between the upflowing and downflowing material to be in their temperature gradients rather than densities.

There are other favorable aspects to the transient heating model. One is that if the coronal heating does increase transiently in a particular flux tube, this would lead to a configuration with mass motions in a loop of

relatively high pressure compared to the surrounding region, which is exactly the geometry required by the limb redshifts observations (Section II). Another is that this model resembles a flare event in that flares can be considered as extreme cases of transient coronal heating. The "well" structure proposed in Figure 1 is similar to that believed to occur in a flare loop (Kane, Frost and Donnelly 1979). Since it is observed that redshifts predominate in flare UV emission (e.g., Underwood et al. 1978), the flare observations support the hypothesis that transient heating will produce more redshifted than blueshifted emission.

If the redshifts are due to transient heating, this implies a strong constraint on theories for coronal heating. The heating must have a large impulsive component. We believe that this would favor models for coronal heating which involve flare-like magnetic-energy release (e.g., Galeev et al. 1981). Hence the observed redshifts of UV line may be providing us with an important clue on the mechanism for coronal heating.

#### Acknowledgments

This work was supported by NASA contracts NGL 05-020-272 and NAGW-92, and ONR contract N00014-75-C-0673.

## REFERENCES

- Antiochos, S. K. 1979, Ap. J. (Letters), 232, 125.
- Antiochos, S. K. 1981, Second Cambridge Workshop on Cool Stars, Stellar Systems and the Sun, Vol. II (Cambridge, MA), p. 115.
- Antiochos, S. K., Emslie, A. G., Shoub, E. C., and An, C.-H. 1982, Ap. J. (submitted).
- Antiochos, S. K., and Krall, K. R. 1979, Ap. J., 229, 788.
- Antiochos, S. K., and Sturrock, P. A. 1978, Ap. J., 220, 1137.
- Antiochos, S. K., and Sturrock, P. A. 1982, Ap. J., 254, 343.
- Athay, R. G. 1981, Ap. J., 249, 340.
- Athay, R. G., and Holzer, T. E. 1982, Ap. J., 255, 743.
- Ayres et al. 1982 (in preparation).
- Borrini, G., and Nocci, G. 1982, Solar Phys., 77, 153.
- Cargill, P. J., and Priest, E. R. 1980, Solar Phys., 65, 251.
- Dere, K. P. 1982, Solar Phys., 77, 77.
- Doschek, G. A., Feldman, U., and Bohlin, J. D. 1976, Ap. J. Lett., 205, L177.
- Doschek, G. A., Feldman, U., Mariska, J. T., and Linsky, J. L. 1978, Ap. J. (Letters) 226, L35.
- Doschek, G. A. and Feldman, U. 1982, Ap. J., 254, 371.
- Feldman, U., Cohen, L., and Doschek, G. A. 1982, Ap. J., 255, 325.
- Galeev, A. A., Rosner, R., Serio, S., and Vaiana, G. S. 1981, Ap. J., 243, 301.
- Gebbie, K. B. et al. 1981, Ap. J. (Letters), 251, L115.
- Glencross, W. M. 1980, Astron. Ap., 83, 65.
- Kane, S. R., Frost, K. J., and Donnelly, R. F. 1979, Ap. J., 234, 669.
- Landini, M., and Monsignori Fossi, B. C. 1981, Astron. Ap., 102, 391.
- Lites, B. W., Bruner, E. C., Chipman, E. G., Shine, R. A., Rottman, G. J., White, O. R., and Athay, R. G. 1976, Ap. J. (Letters), 210, L111.

McClymont, A. N., and Canfield, R. C. 1982, Ap. J. (in press).

Pallavicini, R., Peres, G., Serio, S., Vaiana, G. S., Golub, L., and  
Rosner, R., 1981, Ap. J., 247, 692.

Pneuman, G. W. and Kopp, R. A. 1977, Astron. Ap., 55, 305.

\_\_\_\_\_ 1978, Solar Phys., 57, 49.

Poletto, G. 1981, Solar Phys., 73, 232.

Raymond, J. C., Cox, D. P., and Smith, B. W. 1976, Ap. J., 204, 290.

Raymond, J. C., and Doyle, J. G. 1981, Ap. J., 247 686.

Saxner, M. 1981, Astron. Ap., 104, 240.

Schmahl, E. J., and Orrall, F. Q. 1979, Ap. J. Lett., 231, L41.

Shoub, E. C. 1982, Ap. J. (in press).

Spitzer, L. 1962, Physics of Fully Ionized Gases (2d ed; New York:  
Interscience), Chapt. 5.

Underwood, J. H., Antiochos, S. K., Feldman, U., and Dere, K. 1978, Ap. J.,  
224, 1017.

Vernazza, J. E., Avrett, E. H., and Loesser, R. 1981, Ap. J. Suppl., 45, 635.

Vesecky, J. F., Antiochos, S. K., and Underwood, J. H. 1979, Ap. J., 233, 987.

Zolcinski, M.-C., Antiochos, S. K., Stern, R. A., and Walker, A. B. C. 1982,  
Ap. J., 258, 177.

### Figure Captions

Figure 1 Schematic diagram of the base of a flux tube with higher gas pressure than in the surrounding tubes;  $P_i \gg P_o$ . Observers A and B correspond to viewing the loop when it is near opposite limbs, and C when it is near disk center. Note that A and B would see opposite Doppler shifts from any plasma flow in the tube, which in the diagram is indicated as being downward. Since A can see the loop transition region, he detects redshifts; however, B's view is completely obscured by the surrounding chromosphere and, hence, he does not detect the corresponding blueshifts. Observer C's view is partially obscured so that he detects some redshifts, but also some absorption by neutral hydrogen.

Figure 2 Ratio of the temperature gradient in the downflowing leg to the gradient in the upflowing leg versus temperature, for a steady-state siphon flow model. The model has a mass flux,  $J = 5 \times 10^{-8} \text{ gm cm}^{-2} \text{ sec}^{-1}$ ; momentum flux,  $H = 2 \text{ erg cm}^{-3}$ ; and an energy input rate  $\epsilon = .56 \text{ erg cm}^{-3} \text{ sec}^{-1}$ .

$A_c$

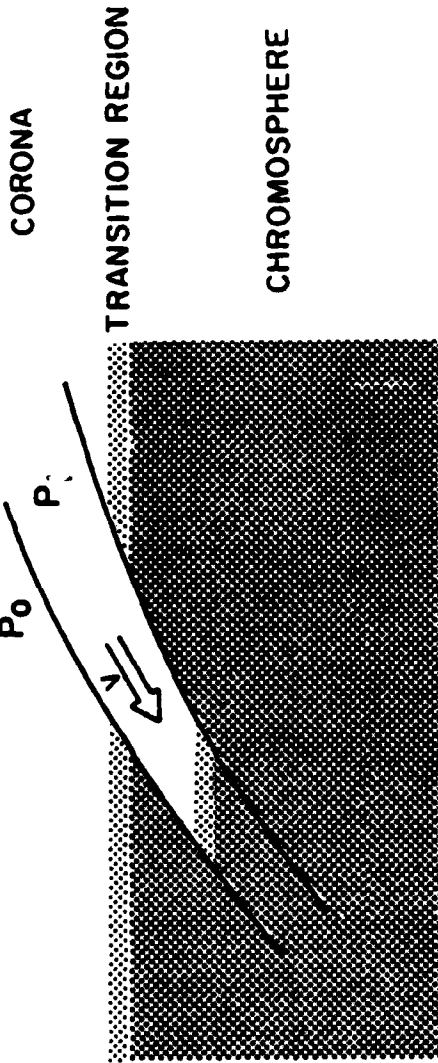


Figure 1

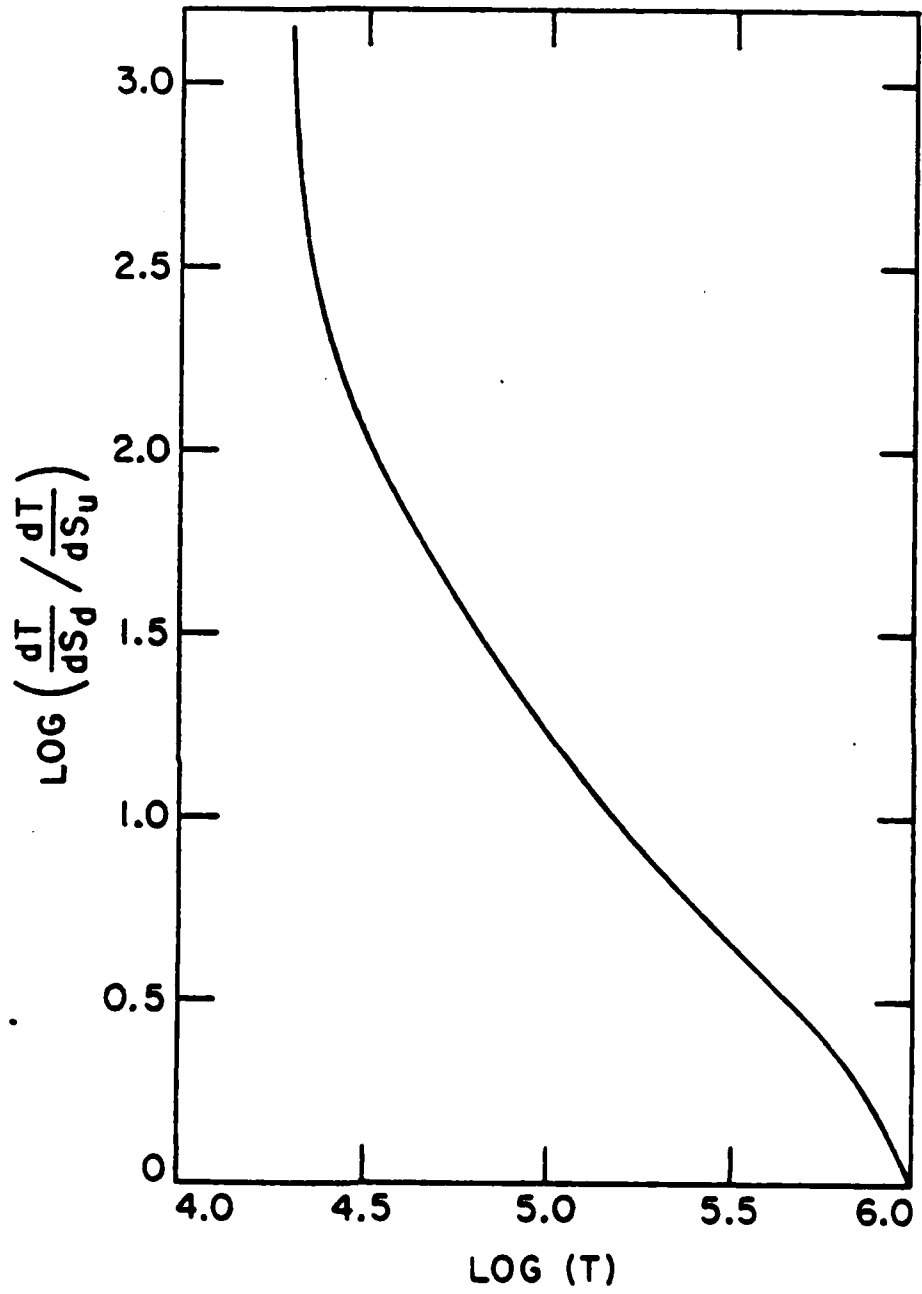


Figure 2